Support Information

High conductive polymer PANI link Bi_2MoO_6 and PBA to establish "Tandem hybrid catalysis system" by coupling photocatalysis and PMS activation technology

Aiwen Wang[1], Rui Wang[1], Yunhao Pan[1], Jiaxin Ni[1], Xiongying Liang[1], Meng Du[1], Jun Zhang[1], Dongmei Liu[1*], Jun Ma[1], Jing Wang[2,3*] and Wei Wang[1*]

[1]State Key Laboratory of Urban Water Resource and Environment (SKLUWRE), School of Environment, Harbin Institute of Technology, Harbin, 150090, P. R. China

[2]Institute of Environmental Engineering, ETH Zürich, Zürich 8093, Switzerland

[3]Laboratory for Advanced Analytical Technologies, Empa, Swiss Federal Laboratories for Materials Science and Technology, Dübendorf 8600, Switzerland

*Corresponding author: Dongmei Liu, Jing Wang, Wei Wang

*E−mail addresses: ldm819@126.com; jing.wang@ifu.baug.ethz.ch; wangweirs@hit.edu.cn;

Texts caption

Text S1. Chemicals and Reagents

In this work, all reagents used in the experiments were analytical grade without further purification. The melamine sponge was obtained from Taobao Alibaba Co., Ltd. Cobalt chloride hexahydrate ($CoCl_2·6H_2O$), potassium ferricyanide($K_3[Fe(CN)_6]$), sodium molybdate dihydrate ($Na_2MoO_4·2H_2O$), doxycycline (DC), tetracycline (TC), chlortetracycline (CTC), oxytetracycline (OTC) hydrochloride, sulfamethoxazole (SMX), sulfonamide (SA), sulfadiazine (SDZ) and levofloxacin (LVF) were purchased from Aladdin Reagent Company, China. Bismuth nitrate pentahydrate ($Bi(NO_3)_3·5H_2O$), N–methyl–2–pyrrolidone, absolute ethanol (EtOH) and Sodium hydroxide (NaOH) were purchased from Tianjin Kermel Chemical Reagent Co. Ltd, China. Sodium citrate ($C_6H_5Na_3O_7$) were purchased from Tianjin Guangfu Fine Chemical Reagent Co. Ltd, China. Ethylene glycol (EG) was purchased from Tianjin Fuyu Fine Chemical Co. Ltd, China. Polyaniline was purchased from Shanghai McLean Biochemical Technology Co. Ltd, China. Deionized water was used throughout all experiments.

Text S2. Preparation

Synthesis of CoFe–PBA PMS activator

CoFe PBA was synthesized by wet chemical precipitation method in previously reported [1]. In a typical experiment, $CoCl_2·6H_2O$ (237.9 mg) and $C_6H_5Na_3O_7$ (658.5 mg) were dissolved in 20 ml of deionized water. Meanwhile, 658.5 mg of $K_3[Fe(CN)_6]$ was also evenly dissolved in 20 mL of deionized water. Then uniformly mix the above solution at 25°C for 12 h. The precipitate was collected, centrifuged and washed several times with deionized water and ethanol, and then dried overnight at 60 °C.

Synthesis of Bi_2MoO_6 photocatalyst

The Bi_2MoO_6 was synthesized by one–step solvothermal reactions in previously reported [2]. In a typical experiment, $Bi(NO_3)_3·5H_2O$ (0.728 g) and $Na_2MoO_4·2H_2O$ (0.182 g) were dissolved in 7.5 ml ethylene glycol, respectively. Then, 45mL EtOH were added to the mixture. After stirring for about 30 minutes, it was transferred to a 100 ml Teflon–lined stainless–steel autoclave and then heated in an electric furnace at 160 °C for 12 h. After heating, the autoclave was cooled down

naturally to room temperature. The precipitate was collected, centrifuged and washed several times with deionized water and ethanol, and then dried overnight at 60 °C.

Establishing tandem hybrid catalysis system

Firstly, 2 mg of PANI was dissolved in 10 mL of N-methyl-2-pyrrolidone (NMP). Then 10 mg of PBA and 10 mg of Bi_2MoO_6 were added to the suspension and dispersed uniformly by ultrasound. Add a sponge to soak it thoroughly, and then dry it in an 80 ℃ oven. Wash and dry repeatedly with water and ethanol. The collected hydrogels were called BiM-PBA@PLS.

Text S3 Characterization

The crystal structure of as–prepared samples was measured using X–ray diffraction (XRD, Bruker D8 Advance diffractometer, Gobel mirror monochromated Cu Kα radiation, λ = 1.54056 Å). Scanning electron microscopy (SEM) was performed with a SIGMA 500 operated at an accelerating voltage of 10 kV. Morphological information was obtained on a Zeiss Neon 40EsV FIBSEM attached with an energy dispersive spectroscopy (EDS). Transmission electron microscopy (TEM) images were obtained with a JEOL 1400 and high–resolution transmission electron microscopy (HRTEM) images were obtained by JEM–2100F instrument with an acceleration voltage of 200 kV. X–ray photoelectron microscopy (XPS) was acquired on a Thermo Escalab 250 using an Al Kα X–ray source and all the binding energies were calibrated using C 1s peak (284.8 eV). The leakage of elements was tested by the Inductively Coupled Plasma Optical–MassSpectrometry (Agilent 7900). TOC analyzer (5000A, Shimadzu) was used to monitor the total organic carbon (TOC) removal. The zeta potential was measured using a Zeta Sizer Nano–ZS system, Nano Series (Malvern, United Kingdom). The UV/Vis diffuse reflectance spectra were recorded by a spectrophotometer (Shimadzu, UV3600), in which $BaSO_4$ was employed as the background. The electron spin resonance (ESR) analysis was conducted with a Bruke emxplus. Photoelectrochemical measurements were recorded using an electrochemical workstation (CHI660E, Chenhua) with a standard three–electrode system. The as–prepared photoelectrode, Pt sheet and Ag/AgCl were used as the working electrode, counter electrode and reference electrode, respectively. All photoelectrochemical measurements were conducted in the Na_2SO_4 solution (0.5 M). Transformation products (TPs) of DC were analyzed by Waters 2695 with Waters ZQ2000. A volume of 10 μL was injected. A C18 column (4.6 × 250 mm,

3 μm particle size) was applied. The binary mobile phase was comprised of 0.1% formic acid aqueous solution (named as solvent a) and acetonitrile (named as solvent b). The elution process was conducted at a flow rate of 0.6 $mL \cdot min^{-1}$.

Text S4. Experimental procedures

Photocatalysis coupling PMS activation technology was evaluated by degradation of DC in aqueous solution under simulated sunlight (300W xenon lamp, AM1.5G), visible light (420 nm cutoff filter) and LED (5w) light. In a typical degradation test, a sponge was dispersed in 50 mL DC aqueous solution, then a certain amount of PMS was added. At regular intervals, 2mL solution was removed and filtered through a 0.22μm polyether sulfone (PES) filter. Then the concentration of residual DC in the reaction solution was immediately determined by UV-visible spectrophotometer at a wavelength of 346 nm. Contrast the synergies of light excitation with and without light.

The used sponges were collected and washed with deionized water and ethanol to remove residual organics for repeatability and stability testing. The initial pH of the reaction solution was not adjusted unless otherwise stated. The desired pH of solutions was achieved by adding 1 mM NaOH or 1 mM H_2SO_4 and measured using a pH meter. Each set of experiments was performed in triplicate and results are reported as the mean of the triplicates. In addition, error bars indicate the reproducibility of data from repeated experiments. The main oxidative species detected by the trapping experiments were $\cdot O_2^-$, ·OH, $SO\cdot_4^-$, holes and $^1O_2$ by using L–ascorbic acid, TBA, MeOH EDTA–2Na and furfural, respectively.

Text S5. Computational details

Density functional theory (DFT) calculation was carried out by Material Studio software packages were used to study the electron density difference and the density of states (DOS), and carried out by CASTEP module within the plane–wave pseudopotential method. The exchange–correlation function was modeled using the generalized gradient approximation (GGA) with Perdew–Burke–Ernzerh (PBE). For the plane–wave basis set, a cutoff of E_{cut} = 517 eV and a 3×3×3 Monkhorst–Pack k–point mesh has been used for the energy calculations. Structural optimization using super–soft pseudopotentials to describe the interaction of valence electrons and nuclei. The convergence criterion for geometric structure optimization is: the convergence thresholds for atomic displacement, interatomic forces, and interatomic internal stress were taken as 0.001 Å, 0.03 eV/Å, and 0.05 GPa,

respectively. The geometric optimization and Fukui function were performed using DMol3 program B3LYP with DNP 3.5 basis set and COSMO's water solvation model. The frontier electron densities of the highest occupied molecular orbital (HOMO) and the lowest unoccupied molecular orbital (LUMO) were used for predicting the molecular reaction sites that the reactive species easily attacked in catalytic system. Besides, Fukui function is a very important concept in conceptual density functional theory, which has been widely used for regioselective prediction of electrophilic, nucleophilic, and radical attacking.

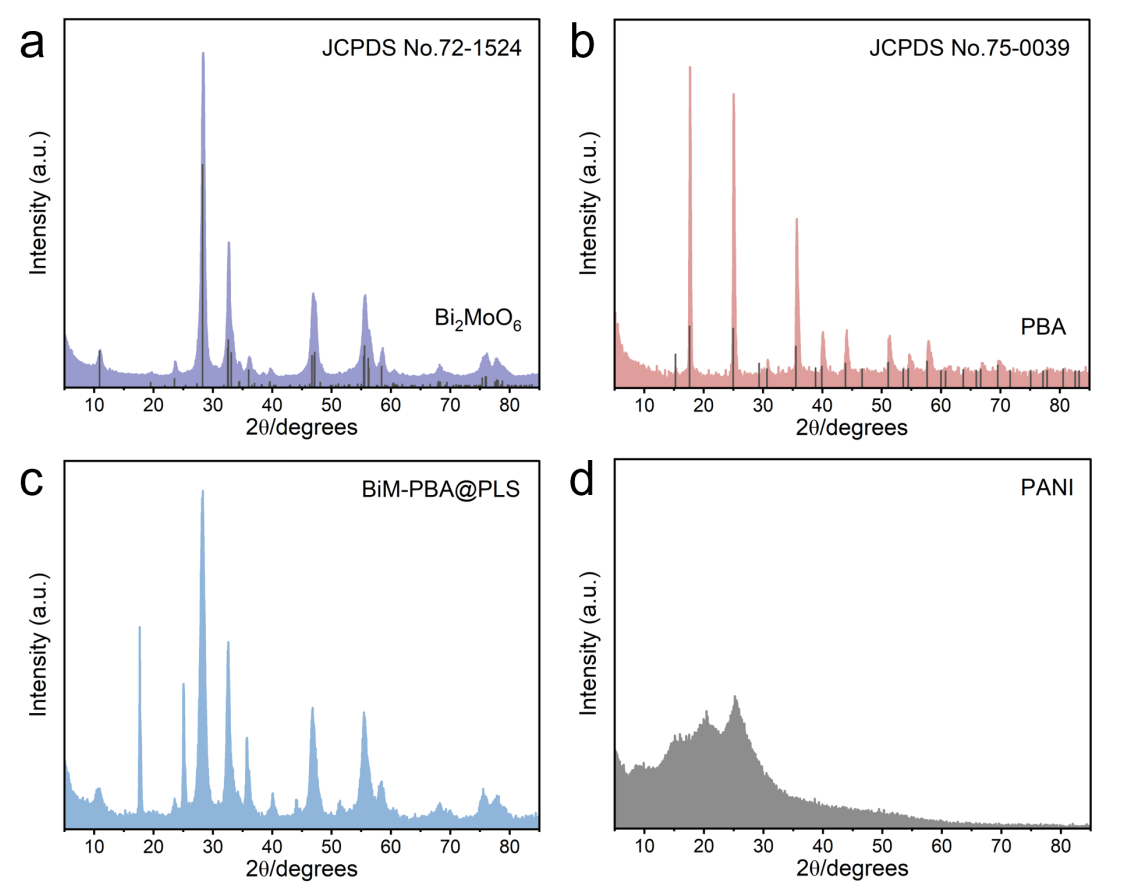

Figure S1. XRD patterns of Bi_2MoO_6 (a), PBA (b), BiM-PBA@PLS (c) and PANI (d).

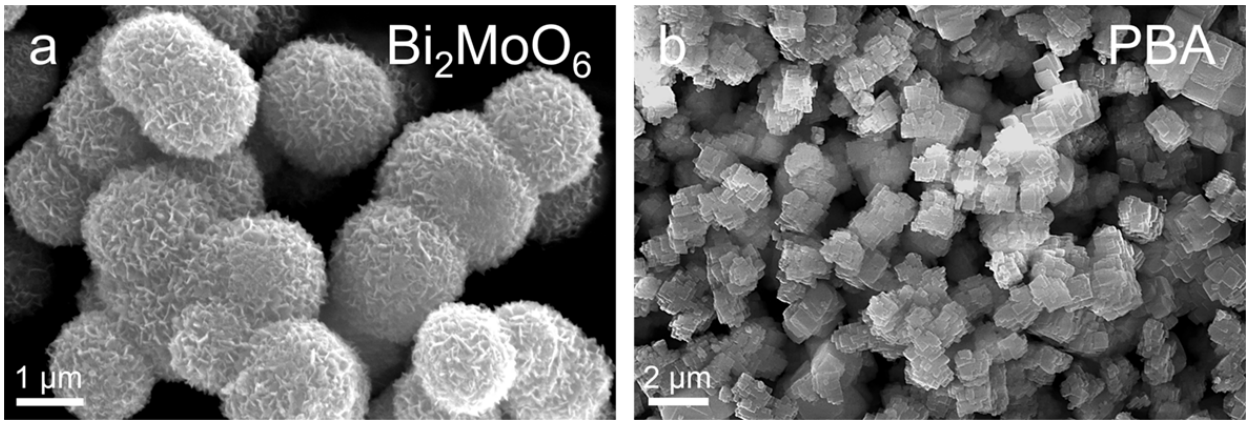

Figure S2. The SEM images of (a) Bi_2MoO_6 and (b) PBA.

Table S1. The analysis of Fourier Transform Infrared spectroscopy of BiM-PBA@PLS.

Wavenumber (cm^{-1})	Characteristic Group
3398	The stretching vibration of O−H and N−H
2099	The stretching vibration of C≡N
1574	The stretching vibration of quinone ring C=C
1484	The stretching vibration of benzene ring C=C
1299	Stretching of aromatic secondary amine C-N
1134	The bending vibration of C-H
842	The stretching vibration of M-O
730	The asymmetrical stretching vibration of M-O
593	The absorption peaks of Fe-CN
551	The absorption peaks of Fe-CN-Co

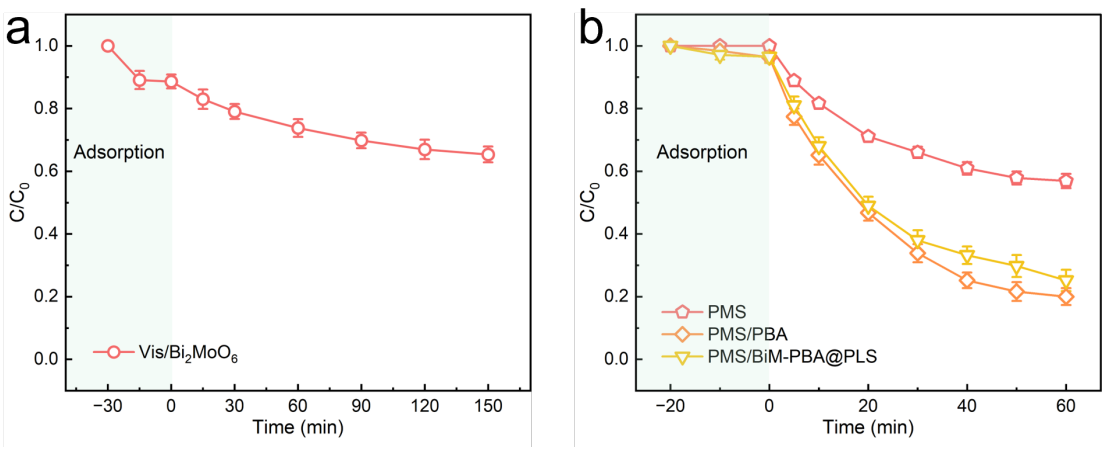

Figure S3. Catalytic degradation curve of as–prepared catalysts.

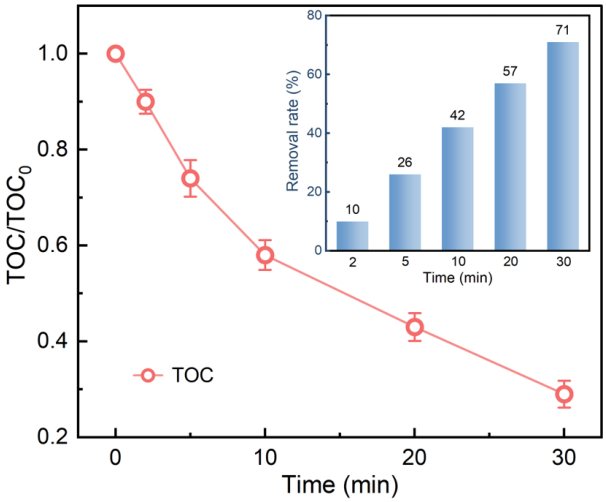

Figure S4. TOC removal ratio during the degradation of DC by BiM-PBA@PLS.

Table S2. Comparison with other photocatalysts in literature.

Photocatalyst	Pollutant	Light source	PMS	Removal Time	k (min^{-1})	Reference
BiM–PBA@PLS	Doxycycline (10 mg L^{-1})	300W XL (λ ≥ 420 nm)	0.200 g L^{-1}	98.02% 30 min	0.1300	This study
$LaFeO_3$/SBA–15	Doxycycline (40 mg L^{-1})	300 W XL (λ ≥ 420 nm)	0.615 g L^{-1}	/	0.0230	[3]
$BiFeO_3$/SBA–15	Doxycycline (40 mg L^{-1})	300 W XL (λ ≥ 420 nm)	1.844 g L^{-1}	/	0.0175	[3]
$BiO_{1-x}Cl$	Doxycycline (50 mg L^{-1})	5 W LED (λ ≥ 400 nm)	0.250 g L^{-1}	79.4% 105 min	0.0062	[4]
$CoCr_2O_4$/α–Fe_2O_3/β–La_2S_3	Doxycycline (10 mg L^{-1})	1000W HL (λ ≥ 420 nm)	/	92.83% 345 min	0.0076	[5]
g–C_3N_4/α–$Bi_2(MoO_4)_3$	Doxycycline (10 mg L^{-1})	500 W XL (λ ≥ 420 nm)	/	93.19% 140 min	0.0183	[6]
In_2O_3/Bi_4O_7	Doxycycline (20 mg L^{-1})	300W XL (λ ≥ 420 nm)	/	92.1% 120 min	0.0197	[7]
AN@CN	Doxycycline (50 mg L^{-1})	300W XL (λ ≥ 420 nm)	/	98.67% 60 min	0.0405	[8]
BiM/ZnC@PANI	Doxycycline (10 mg L^{-1})	300W XL (λ ≥ 420 nm)	/	90% 150 min	0.0119	[2]
ILDAc/MIL–68(In)–NH_2	Doxycycline (10 mg L^{-1})	500 W XL (λ ≥ 420 nm)	/	92% 180 min	0.0092	[9]
$Bi_7O_9I_3$/g–C_3N_4	Doxycycline (20 mg L^{-1})	300W XL (λ ≥ 420 nm)	/	80% 120 min	0.0125	[10]
BiOBr/$FeWO_4$	Doxycycline (20 mg L^{-1})	300 W XL (λ ≥ 420 nm)	/	90.4% 60 %	0.0375	[11]
Nd–BiO_{2-x}	Doxycycline (10 mg L^{-1})	300 W XL (λ ≥ 420 nm)	/	86.14% 120 min	0.0134	[12]
MnO/CoO/WO_3	Doxycycline (20 mg L^{-1})	/	0.100 g L^{-1}	80.04% 120 min	0.0471	[13]
CuO/Fe_2O_3	Doxycycline (50 mg L^{-1})		0.050 g L^{-1}	92.6% 120 min	0.0434	[14]

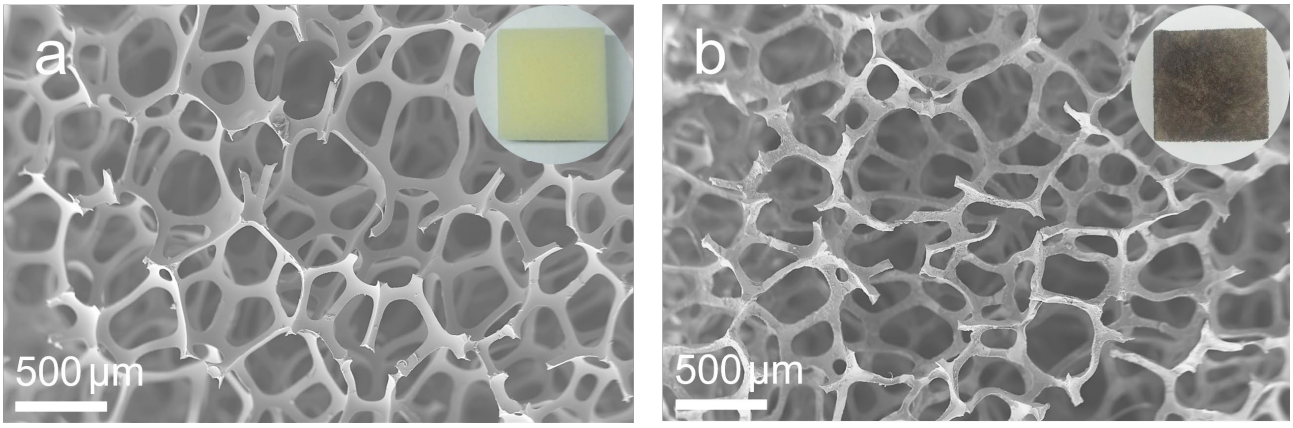

Figure S5. The SEM images and (inset) photos of (a) sponge and (b) BiM-PBA@PLS.

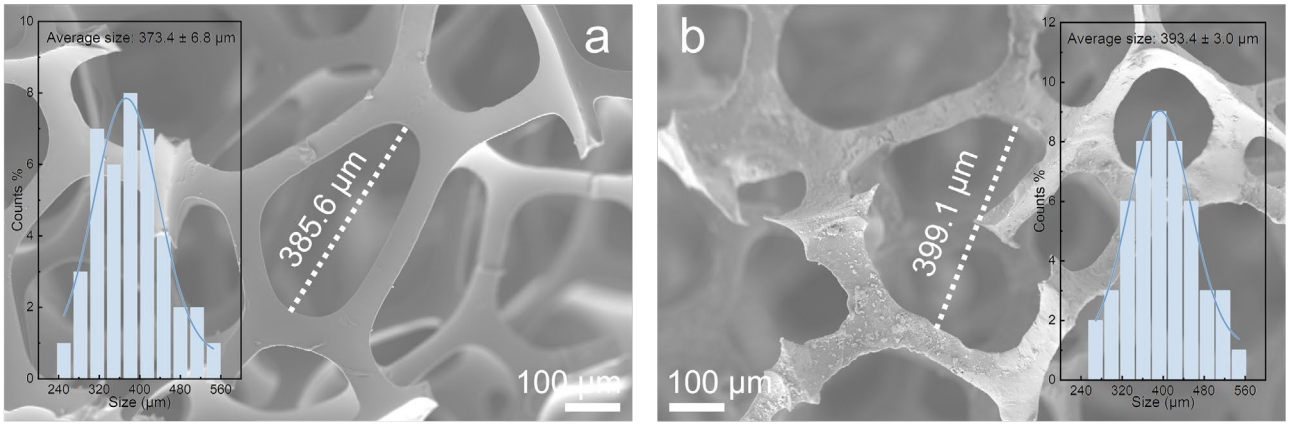

Figure S6. The SEM image and size distribution of (a) sponge and (b) BiM-PBA@PLS

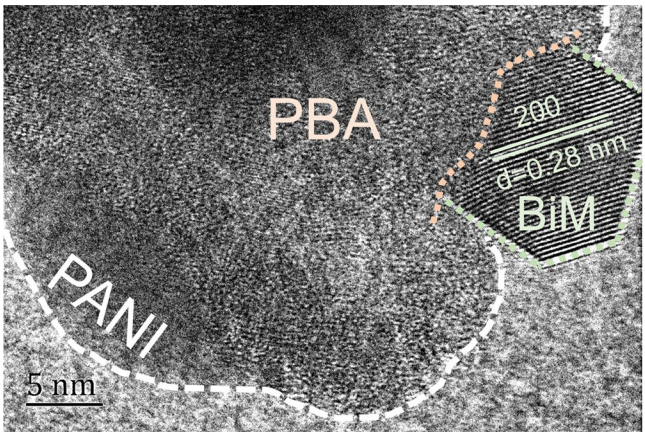

Figure S7. The HRTEM image of BiM−PBA@PLS.

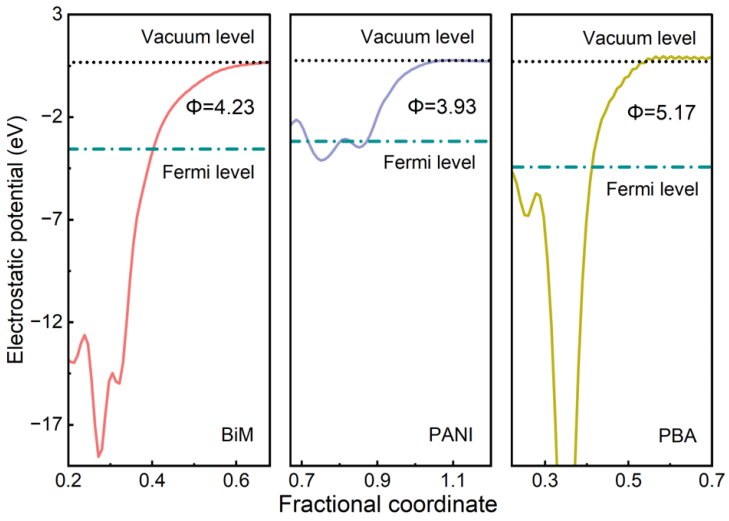

Figure S8. Electrostatic potentials of as–prepared catalysts.

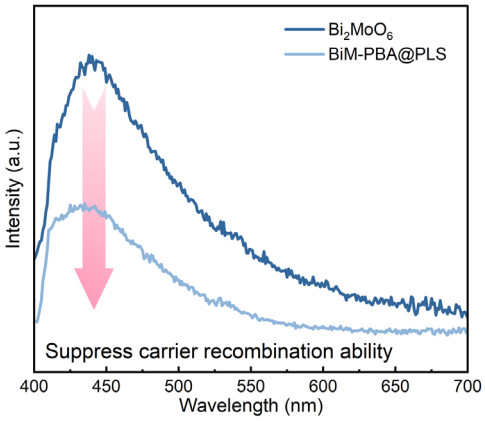

Figure S9. PL characterizations of Bi_2MoO_6 and BiM–PBA@PLS.

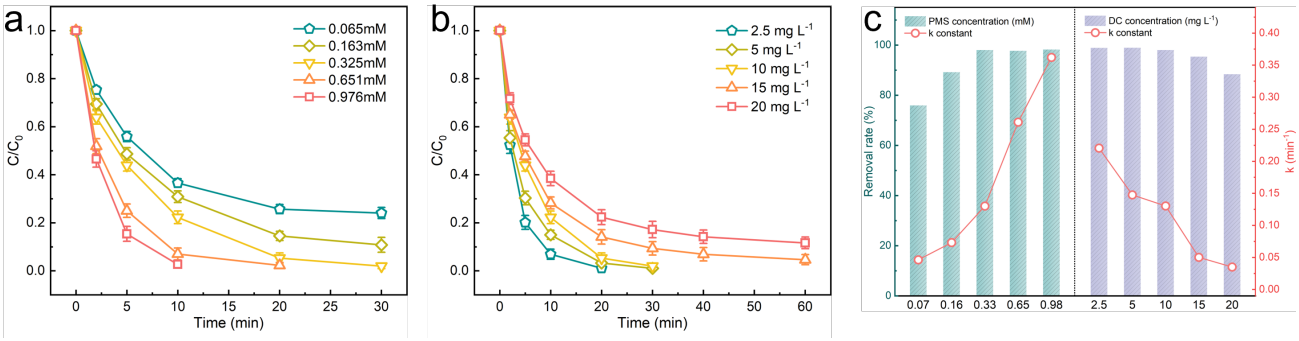

Figure S10. Catalytic degradation curve of different (a) PMS concentration and (b) DC concentration. (c) Difference of removal rate and apparent reaction rate constant k.

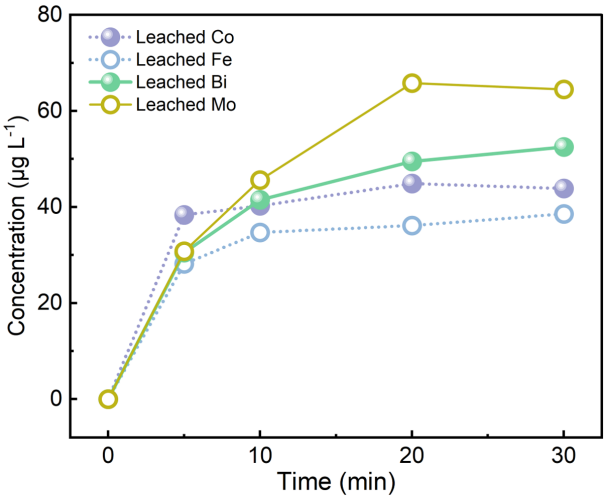

Figure S11. Leakage of Co, Fe, Bi and Mo elements into aqueous solution.

Table S3. Leakage of ions (Co, Fe Bi and Mo) of catalysts into aqueous solution after photocatalytic degradation of DC.

($\mu g\ L^{-1}$)	5 min	10 min	20 min	30 min
Leached [Co]	38.365	40.254	44.897	43.871
Leached [Fe]	28.156	34.689	36.129	38.554
Leached [Bi]	30.5	41.5	49.5	52.5
Leached [Mo]	30.8	45.6	65.8	64.5

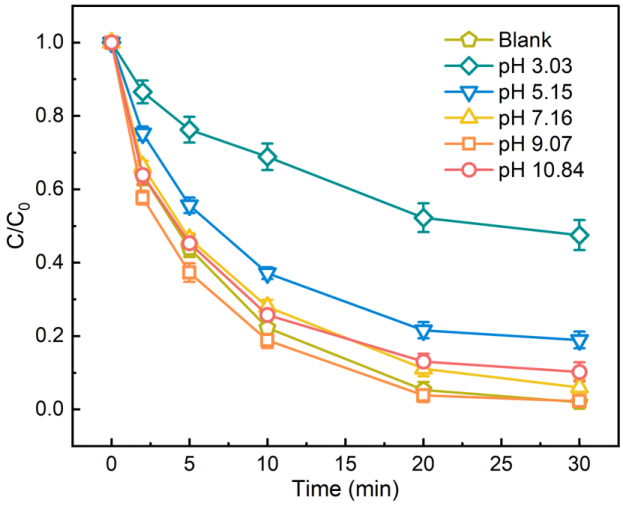

Figure S12. Catalytic degradation curve of different pH with photoexcitation.

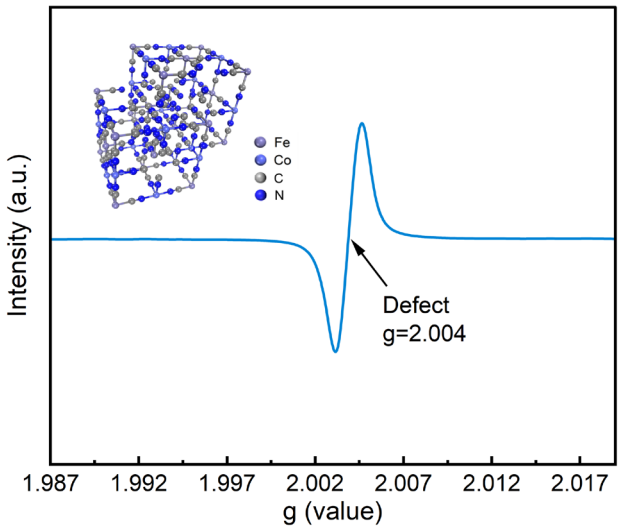

Figure S13. EPR spectra of as–prepared catalysts.

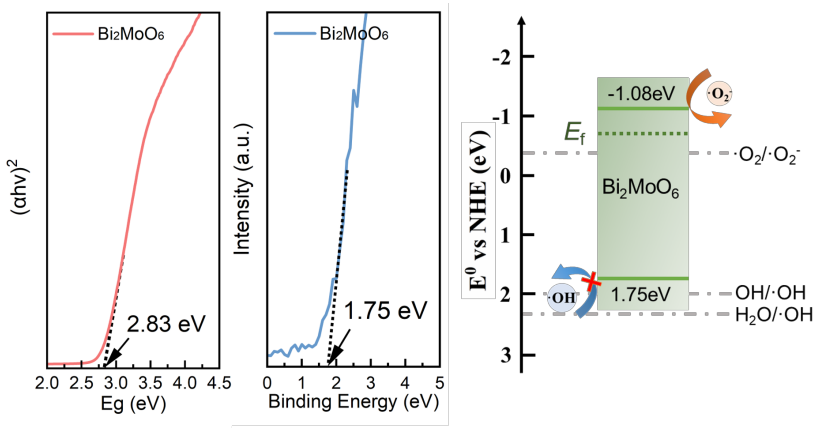

Figure S14. VB XPS spectra and the corresponding band gap of as–prepared Bi_2MoO_6.

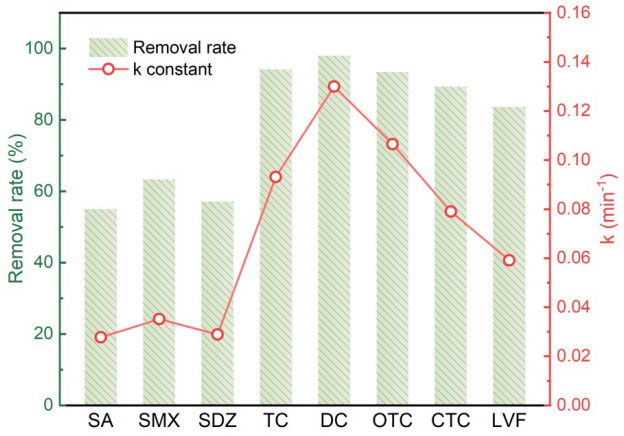

Figure S15. Degradation of three typical antibiotics, sulfonamides (SA, SMX and SDZ), tetracyclines (TC, DC, OTC and CTC) and quinolones (levofloxacin LVF) by BiM-PBA@PLS, respectively. Reaction Conditions: [concentration] = 10 mg L^{-1}, [PMS] = 0.325 mM.

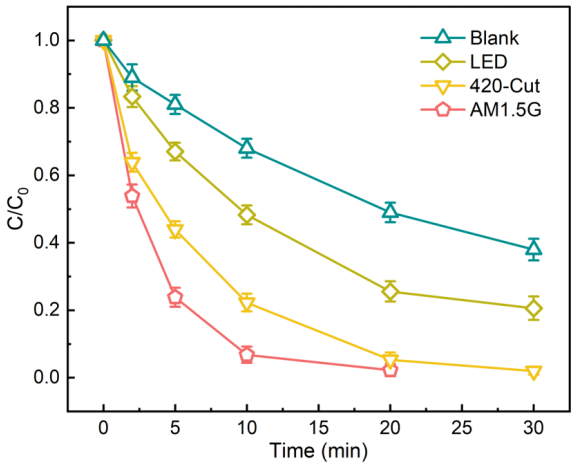

Figure S16. The degradation of DC under different illuminant.

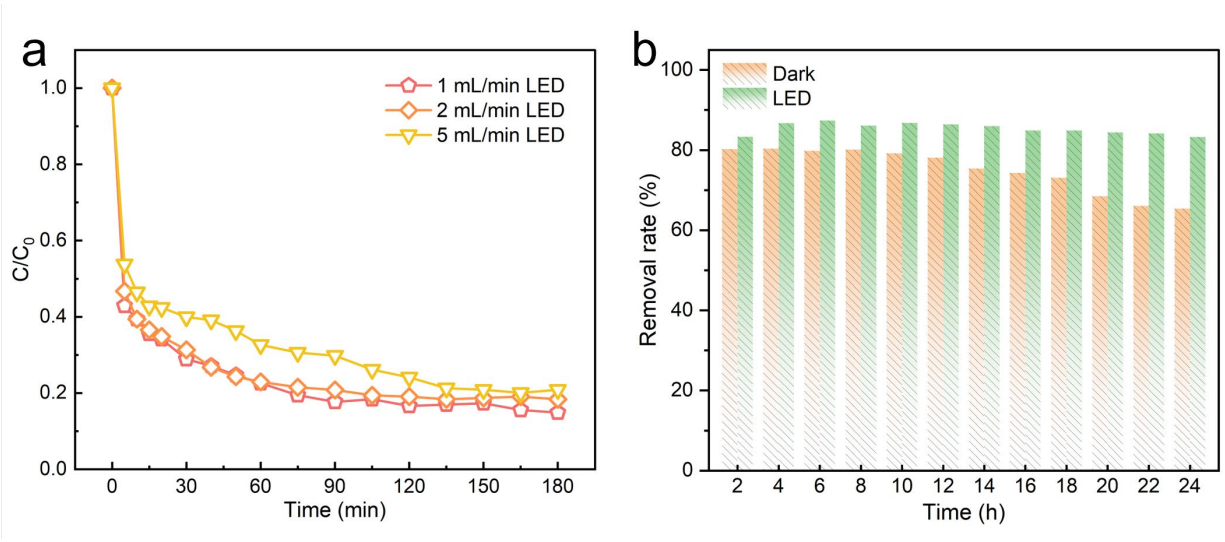

Figure S17. Performance of BiM-PBA@PLS in continuous flow equipment.

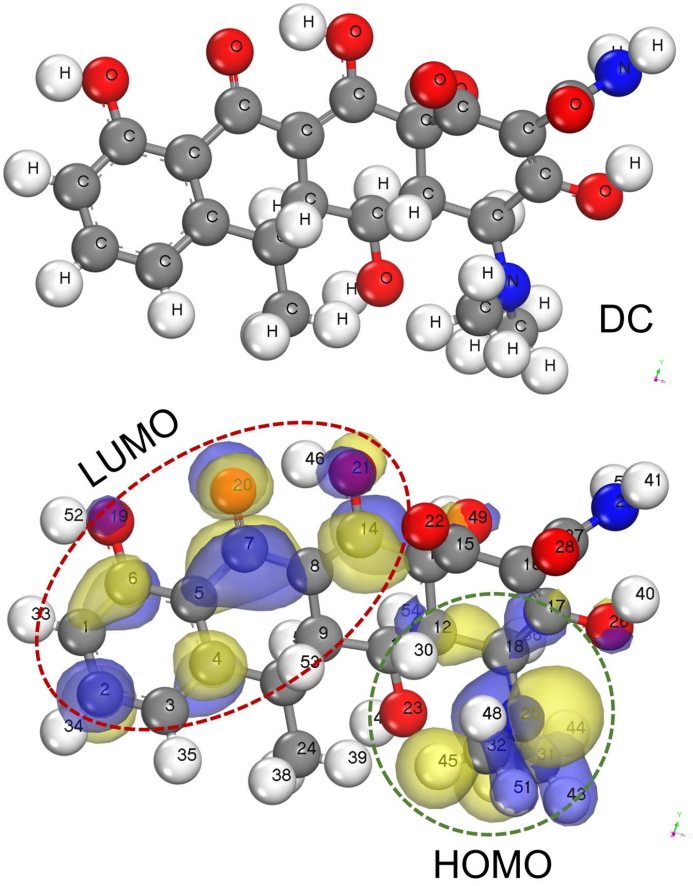

Figure S18. The HOMO and LUMO of DC.

Table S4. Calculated Fukui index of DC.

No.	Atom	f^- (Electrophilic)	f^+ (Nucleophilic)	f^0 (Radical)
1	C	0.003	0.034	0.018
2	C	0.003	0.069	0.036
3	C	0.002	0.030	0.016
4	C	0.001	0.039	0.020
5	C	0.001	0.028	0.015
6	C	0.002	0.044	0.023
7	C	0.004	0.120	0.062
8	C	0.004	0.030	0.017
9	C	0.003	0.006	0.004
10	C	0.000	0.006	0.003
11	C	0.002	0.004	0.003
12	C	0.012	0.001	0.007
13	C	0.006	0.009	0.007
14	C	0.001	0.075	0.038
15	C	0.007	0.005	0.006
16	C	0.018	0.003	0.011
17	C	0.005	0.004	0.005
18	C	0.023	0.002	0.012
19	O	0.002	0.031	0.017
20	O	0.007	0.123	0.065
21	O	0.006	0.064	0.035
22	O	0.027	0.013	0.020
23	O	0.000	0.008	0.004
24	C	0.004	0.006	0.005
25	N	0.241	0.002	0.121
26	O	0.019	0.006	0.013
27	C	0.007	0.002	0.004
28	O	0.018	0.005	0.011
29	N	0.007	0.002	0.005
31	C	0.058	0.001	0.030
32	C	0.054	0.001	0.027
49	O	0.009	0.024	0.017

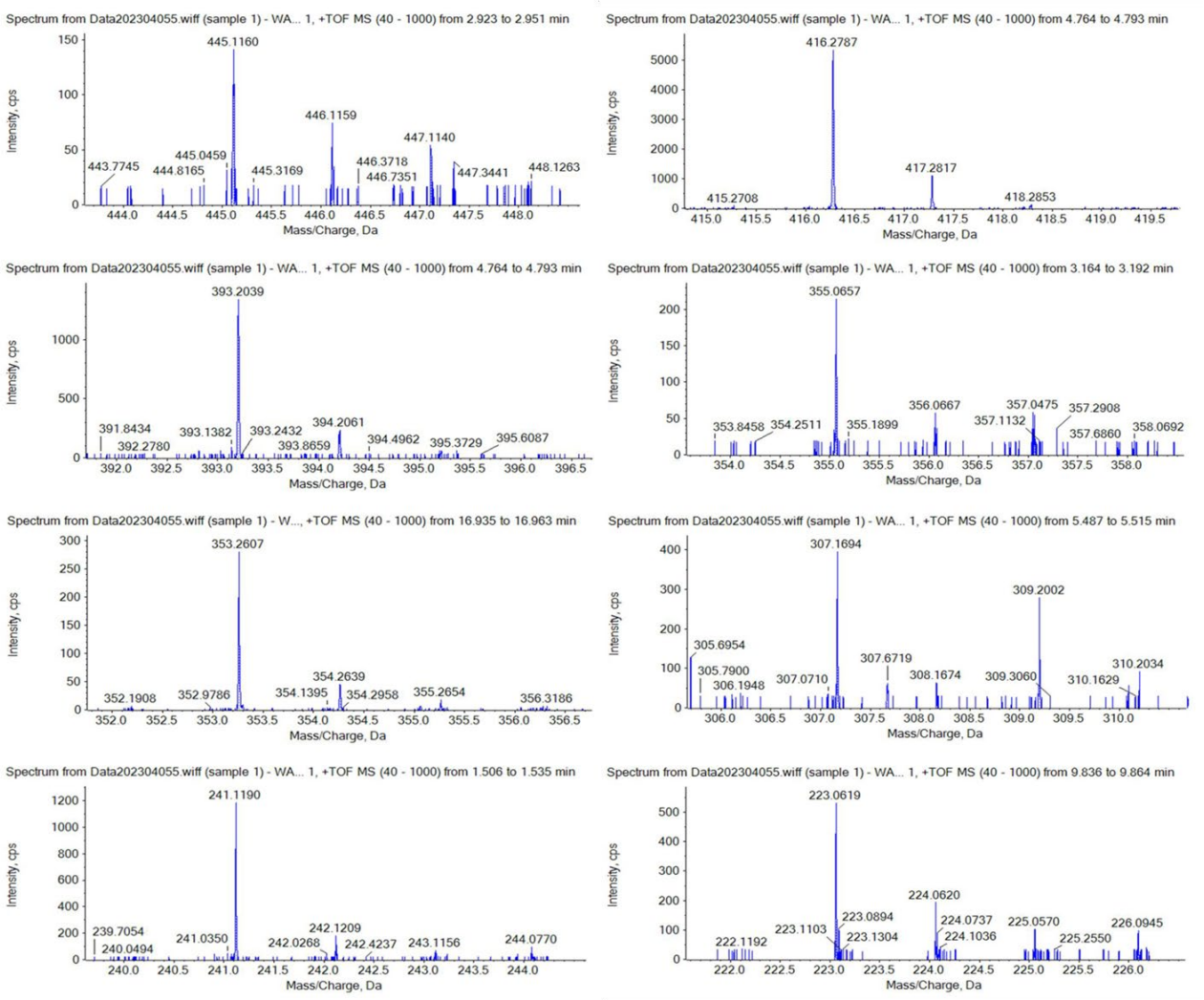

Figure S19. Fragment ions and oxidation products in identification of DC in the catalytic system.

Table S5. The structural information of the possible intermediate products.

Name	Observed *m/z*	Formula	Proposed structure
DC	445	$C_{22}H_{24}N_2O_8$	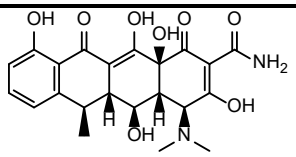
D1	417	$C_{20}H_{20}N_2O_8$	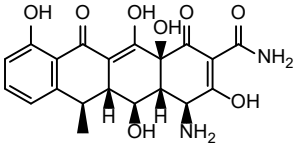
D2	416	$C_{20}H_{17}NO_9$	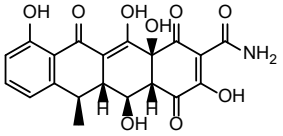
D3	355	$C_{21}H_{26}N_2O_3$	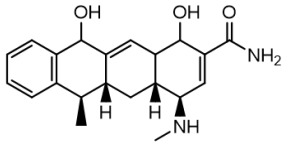
D4	393	$C_{19}H_{20}O_9$	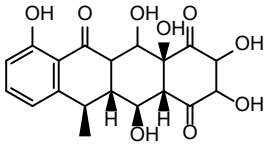
D5	353	$C_{20}H_{16}O_6$	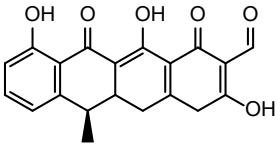
D6	307	$C_{17}H_{22}O_5$	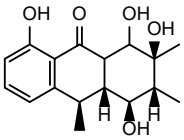
D7	241	$C_{15}H_{12}O_3$	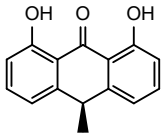
D8	223	$C_{12}H_{14}O_4$	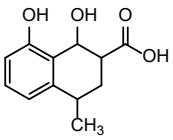

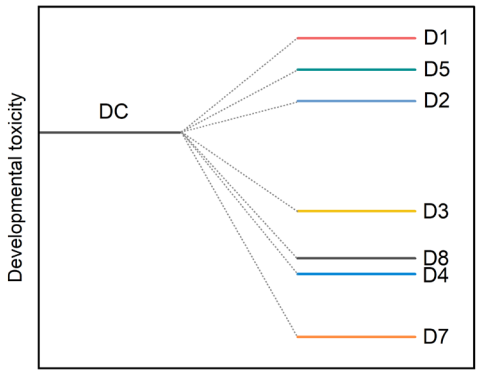

Figure S20. Theoretical calculated developmental toxicity of DC and their degradation intermediates.

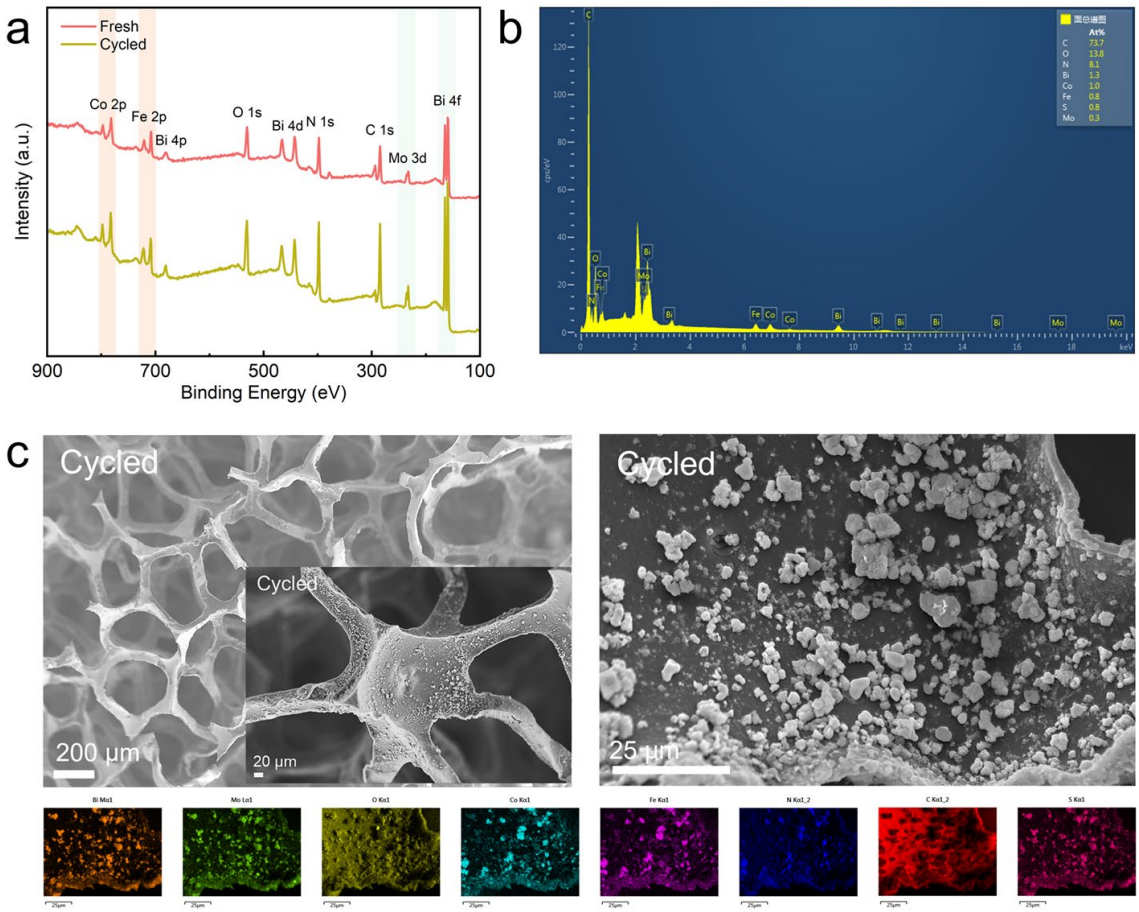

Figure S21. The XPS spectra (a), EDS spectrum (b), SEM and mapping (c) of BiM−PBS@PLS after cycling.

Reference:

[1] L.-L. Gu, J. Gao, C. Wang, S.-Y. Qiu, K.-X. Wang, X.-T. Gao, K.-N. Sun, P.-J. Zuo, X.-D. Zhu, Thin-carbon-layer-enveloped cobalt–iron oxide nanocages as a high-efficiency sulfur container for Li–S batteries, Journal of Materials Chemistry A, 8 (2020) 20604-20611.

[2] A. Wang, W. Wang, J. Ni, D. Liu, D. Liu, J. Ma, X. Jia, MOF derived ZnO clusters on ultrathin Bi_2MoO_6 yolk@shell reactor: Establishing carrier transfer channel via PANI tandem S–scheme heterojunction, Applied Catalysis B: Environmental, 328 (2023) 122492.

[3] Q. Zhao, M. Long, H. Li, Q. Wen, D. Li, Synthesis of $MFeO_3$/SBA-15 (M = La or Bi) for peroxymonosulfate activation towards enhanced photocatalytic activity, New Journal of Chemistry, 46 (2022) 1144-1157.

[4] M. Liu, H. Qin, H. Xu, Z. Zou, C. Deng, D. Xia, Q. Yu, Y. Zheng, D. Chen, Confine activation peroxymonosulfate by surface oxygen vacancies of BiO1−xCl to boost its utilization rate, Separation and Purification Technology, 307 (2023) 122711.

[5] P.R. Sivaranjani, A. Syed, A.M. Elgorban, A.H. Bahkali, R. Balakrishnaraja, R.S. Varma, S. Sudheer Khan, Fabrication of ternary nano-heterojunction via hierarchical deposition of α-Fe_2O_3 and β-La_2S_3 on cubic $CoCr_2O_4$ for enhanced photodegradation of doxycycline, Journal of Industrial and Engineering Chemistry, 118 (2023) 407-417.

[6] V. Vasanthakumar, M. Alsawalha, T. Alomayri, S. Allehyani, Y.-b. Hu, M.-L. Fu, B. Yuan, α-$Bi_2(MoO_4)_3$ nanorods decorated with two-dimensional g-C_3N_4 nanosheets for efficient degradation of doxycycline under visible light illumination, Process Safety and Environmental Protection, 163 (2022) 1-13.

[7] Z. Pan, L. Qian, J. Shen, J. Huang, Y. Guo, Z. Zhang, Construction and application of Z-scheme heterojunction In_2O_3/Bi_4O_7 with effective removal of antibiotic under visible light, Chemical Engineering Journal, 426 (2021) 130385.

[8] C. Feng, Y. Deng, L. Tang, G. Zeng, J. Wang, J. Yu, Y. Liu, B. Peng, H. Feng, J. Wang, Core-shell Ag_2CrO_4/N-GQDs@g-C_3N_4 composites with anti-photocorrosion performance for enhanced full-spectrum-light photocatalytic activities, Applied Catalysis B: Environmental, 239 (2018) 525-536.

[9] D. Li, T. Hua, X. Li, J. Cheng, K. Du, Y. Hu, Y. Chen, In-situ fabrication of ionic liquids/MIL-68(In)–NH_2 photocatalyst for improving visible-light photocatalytic degradation of doxycycline hydrochloride, Chemosphere, 292 (2022) 133461.

[10] Z. Zhang, Z. Pan, Y. Guo, P.K. Wong, X. Zhou, R. Bai, In-situ growth of all-solid Z-scheme heterojunction photocatalyst of $Bi_7O_9I_3$/g-C_3N_4 and high efficient degradation of antibiotic under visible light, Applied Catalysis B: Environmental, 261 (2020).

[11] J. Gao, Y. Gao, Z. Sui, Z. Dong, S. Wang, D. Zou, Hydrothermal synthesis of BiOBr/$FeWO_4$ composite photocatalysts and their photocatalytic degradation of doxycycline, J. Alloy. Compd., 732 (2018) 43-51.

[12] Q. Wang, D. Xu, Y. Dong, S. Pang, L. Zhang, G. Zhang, L. Lv, X. Liu, Y. Xia, L.C. Campos, Z. Ren, P. Wang, Unsaturated Nd-Bi dual-metal sites enable efficient NIR light-driven O_2 activation for water purification, Applied Catalysis B: Environmental, 319 (2022) 121924.

[13] X. Luo, Y. You, M. Zhong, L. Zhao, Y. Liu, R. Qiu, Z. Huang, Green synthesis of manganese–cobalt–tungsten composite oxides for degradation of doxycycline via efficient activation of peroxymonosulfate, Journal of Hazardous Materials, 426 (2022) 127803.

[14] X. Luo, T. Asefa, R. Qiu, C. Su, L. Cui, Z. Huang, Robust Adsorption and Persulfate-Based Degradation of Doxycycline by Oxygen Vacancy-Rich Copper-Iron Oxides Prepared through a Mechanochemical Route, ACS ES&T Water, 2 (2022) 1031-1045.